Contents lists available at ScienceDirect

Sensors and Actuators A: Physical

journal homepage: www.elsevier.com/locate/sna

Micromachined plastic W-band bandpass filters

Firas Sammoura*, Yiin-Kuen Fuh, Liwei Lin

Department of Mechanical Engineering, University of California at Berkeley, Berkeley, CA 94720-1740, USA

A R T I C L E   I N F O

Article history:
Received 4 November 2007
Received in revised form 2 March 2008
Accepted 3 March 2008
Available online 13 March 2008

Keywords:
RF-MEMS
Microwave engineering
Millimeter waves
Plastic hot embossing
GHz
Iris filters
Electroplating

A B S T R A C T

Results are presented for micromachined plastic waveguide bandpass iris filters for W-band applications using a cost-effective polymer micro hot embossing process in conjunction with metallic electroplating and sealing techniques. The prototype filter has an 8-μm thick electroplated gold layer on a polymeric WR-10 waveguide with a 5-cavity Chebyschev-type design. Measurement results show center frequency of 96.77 GHz with a bandwidth of 3.15%, a loaded quality factor 31.73 and an unloaded quality factor for a single cavity resonator is 1210.6, respectively. A minimum insertion loss of −1.22 dB and return loss of better than −9.3 dB have been measured over the entire passband.

1. Introduction

Metallic waveguide (hollow pipe type) filters fabricated by precision mechanical machining processes have been widely used in high power wireless applications because of their low loss and high power handling capabilities [1]. In recent years, micromachined three-dimensional (3D) processes *have been demonstrated to make coaxial transmission lines* to construct high frequency components, including filters [2]. For example, Chen et al. have demonstrated a compact, low-loss Ka-band filter using coaxial line architecture but the fabrication process requires forty-one layers [3]. Asao et al. have shown a metal-plated plastic waveguide filter using injection molding for Ka-band applications [4]. Chi and Rebeiz have reported a planar inter-digitated bandpass filter operating at 20 GHz using silicon-based micromachining processes [5]. Robertson et al. have presented a membrane supported W-band bandpass filter using a 5-element, coupled microstrip line in shielded cavity [6]. Jiang et al. have made Ka-band filter using an SU-8 UV lithography and assembly process [7]. In addition, Lee et al. have fabricated perfluorocyclobutane (PFCB) optical waveguides of 41 μm × 47 μm cross-section using a PDMS molding process [8]. These previous works show examples of innovative processes and materials to make various filters. Here, we present a different class of micromachined filters based on hollow waveguides with a cost-effective hot embossing and electroplating process. Hot embossing process is chosen over injection molding in this work as hot embossing is less expensive for low-volume research demonstration. Furthermore, our group has extensive experiences in the hot embossing process [9–11]. The filters are designed by constructing resonant cavities inside the polymeric hollow waveguide with a coated metal layer. Integrated plastic flanges have also been fabricated and connected to these filters by press fitting as the matching connectors between the filters and network analyzer during the experimental characterization processes.

2. Design of iris filters

Fig. 1(a) shows the schematic diagram of a 5-cavity iris filter. Theoretically, resonant cavities are separated by metal irises that have no thickness. The inductive metal planes can be modeled as parallel inductive shunts connected between transmission lines of various electrical lengths and the conductance of the inductive irises can be approximated [12] when the metal iris thickness is much smaller than the operating wavelength. The insertion loss method of a Chebyshev type design is used to synthesize the passband and stop-band responses [13]. We chose a 5-cavity iris filter design in the prototype demonstration after considering trade-offs between design simplicity and performance. For example, increasing number of cavities results in steeper cutoff (out-of-band rejection) but complicates the design and fabrication issues with possible additional insertion losses from imperfections. In this paper, the design is symmetric in geometry and the resonant lengths are represented as R_1, R_2, and R_3, respectively, while the iris gaps are represented as d_1, d_2, and d_3, respectively. It is noted that

* Corresponding author. Tel.: +1 510 684 9966; fax: +1 510 642 6163.
E-mail address: firas.sammoura@analog.com (F. Sammoura).

0924-4247/$ – see front matter © 2008 Elsevier B.V. All rights reserved.
doi:10.1016/j.sna.2008.03.005

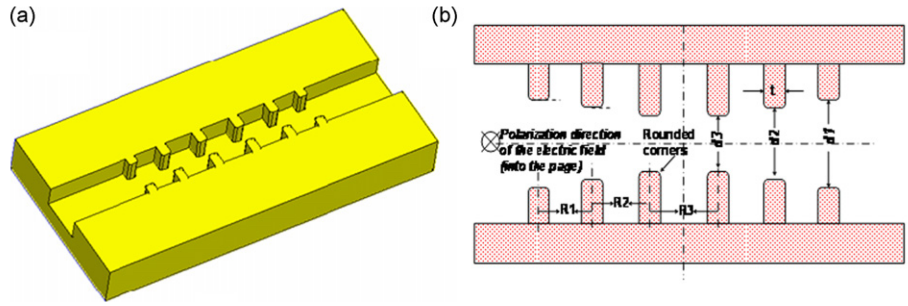

Fig. 1. (a) Schematic top-view diagram of a 5-cavity iris filter. (b) Top view of the filter to be manufactured by the plastic molding process. R_1, R_2, and R_3 are resonant lengths while d_1, d_2, and d_3 are the gaps of irises. The thickness of iris is designated as "t".

the irises have thickness, t, as determined mainly by the limitation of the machining process in making the mold inserts and the electroplating process also adds extra thickness. Furthermore, rounded corners on the irises have been drawn to reflect the practical limitation in the electric discharge machining (EDM) process.

The prototype iris filter was designed to have a ripple level of 0.01 dB for an operation center frequency near 95 GHz based on the previous plastic waveguide work [14]. However, the theoretical formula assumes negligible iris thickness while fabricated filters have finite iris thickness. Simulations are performed using HFSS (High Frequency Structure Simulator) by Ansoft Corp. to characterize the effects of the iris thickness on the bandwidth and center frequency in order to optimize the filter design as illustrated in Fig. 2. If the thickness of the iris is small such as 100 μm, the theoretical model (irises with no thickness) predicted a center frequency of 81.9 GHz with a bandwidth of 8 GHz but the simulation result shows a center frequency of 84.9 GHz with a bandwidth of 7.5 GHz. If the iris thickness increases to 300 μm, the simulation result indicates center frequency of 88.9 GHz and with a bandwidth of 5.3 GHz. If the iris thickness is 550 μm, the center frequency and the bandwidth are 94.9 GHz and 3.7 GHz, respectively. It is noted that as the iris thickness increases, the center frequency shifts to a higher value and the bandwidth reduces while the penalty is the reduction in the return loss.

Simulations are performed to characterize the effects of the round corners as illustrated in Fig. 3. It is observed that irises of 0.3 mm in thickness and rounded edges with radius of 0.125 mm can cause central frequency shift from 88.3 GHz to 85.2 GHz while the bandwidth and return loss remain almost the same. This can be explained that the rounded irises have smaller effective thickness and consequently cause frequency responses to move lower.

3. Fabrication and measurement results

A plastic micromachining process by means of hot embossing and selectively electroplating and sealing [14] has been used to make these filters. However, in contrast to the previous work by using conventional mechanical machining tools and aluminum as the mold insert, electric discharge machining (EDM) is applied to create iris structures as conventional milling tools cannot achieve the required fine iris dimension and steel is used as the mold insert for better strength during the molding process on fine features. The EDM process can achieve tens of μm features depending on the diameter of the wires. Topas®COC 8007 is used as the base polymeric material and a silicon top cover is adopted in the prototype to enclose and complete the hollow waveguide structure. Topas®COC has superior properties than some of the other polymeric materials in chemical stability such as less absorption of water, chemically inert to acetone and isopropanol. Furthermore, as a proof-of-concept demonstration, device operation is conducted at room temperature while issues on thermal mismatch will require further investigations for device operations under various environments. The system is selectively electroplated with an 8 μm-thick gold layer over the inner surfaces of the waveguide. The electroplating process also seals the silicon cover and the plastic substrate [15]. The skin depth of electromagnetic wave at around 95 GHz is 1.33 μm by using 4-point probe measured conductivity value of $1.5 \times 10^6\ \Omega\,\mathrm{m}^{-1}$ and the 8-μm thick gold layer is more than 6 times of skin depth to function as the inner reflection surface.

Fig. 4(a) shows SEM micrograph of the steel mold insert where iris-shapes are fabricated by EDM. It is noted that these irises have round instead of sharp tips as the 125 μm in radius EDM thread has been used to make the mold insert. The black spots on the mold insert surface are charged-up (by electrons in SEM) residual plastic particles. One prototype device is forcefully broken on

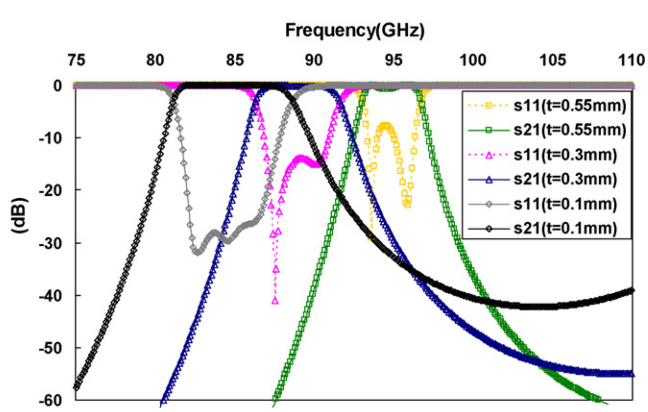

Fig. 2. HFSS simulations showing the effect of iris thickness to the bandwidth and center frequency.

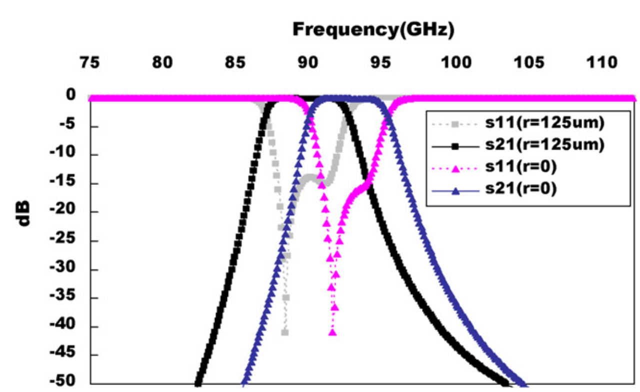

Fig. 3. HFSS simulations showing the effect of rounded iris corners due to EDM process.

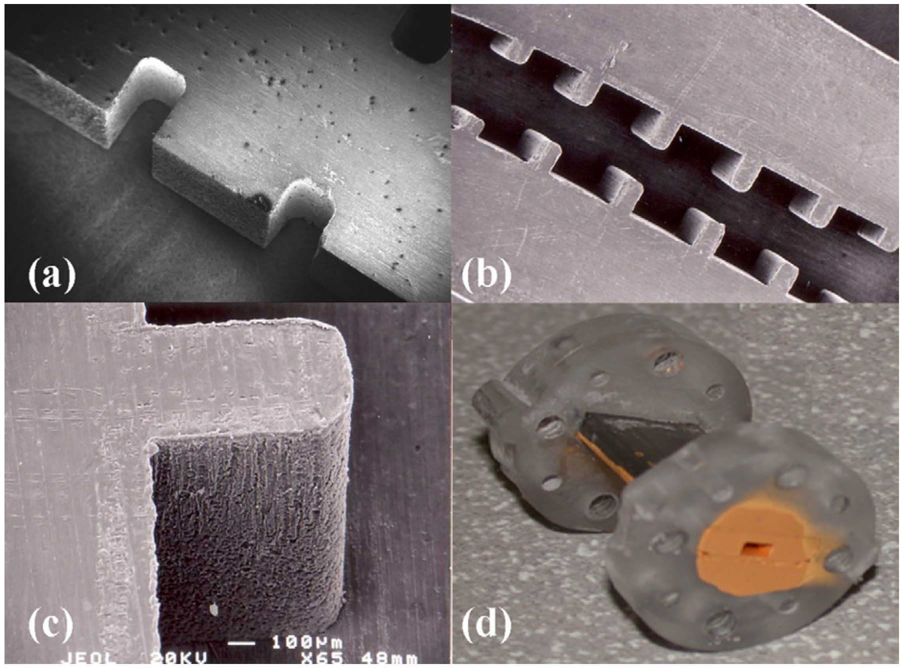

Fig. 4. SEM microphoto of: (a) the steel mold insert; (b) the fabricated plastic iris filter after it is forcefully broken on purpose for examinations. (c) A close-up view of the iris. (d) Optical photo of the fabricated iris filter with two adaptors.

purpose for the SEM session as shown in Fig. 4(b). The close view SEM micrograph in Fig. 4(c) illustrates good replication including round corners. It is also noted that the electroplating process penetrates about 250 μm deep inside the sealing line [15] such that traces of electroplated gold can be observed in both Fig. 4(b) and (c). This effect comes from non-perfect sealing during the electroplating process and could be leakage sources if the gold layer does not completely seal the waveguide. Our experiences show that the 8-μm thick gold deposition is enough to overcome this potential problem by sealing the interfacial regions properly. Fig. 4(d) is an optical photograph of the plastic iris filter with integrated plastic adaptors at both ends for easily connection with the network analyzer. The dimensions of the adaptor follow the specifications used in the conventional waveguides [14].

Two prototype iris filters have been fabricated by using two different mold inserts (fabricated by different EDM conditions) and tested and their dimensions have been measured (Optical Comparator by MicroVu Corporation). Table 1 shows the design, mold insert, and fabricated plastic filter dimensions where measurements uncertainty is ±20 μm. It is noted that the mold insert dimensions are within 10 μm of the design values and the only exception is the iris thickness. This dimension is dominated by the precision of the micro EDM process and the error can be as big as 70 μm in the second prototype. The coefficient of thermal expansion of Topas®COC and steel are $60 \times 10^{-6}\,^{\circ}C^{-1}$ and $13 \times 10^{-6}\,^{\circ}C^{-1}$

Table 1
Filter parameter dimensions

Parameter	Design	Mold insert		Fabricated Filter	
		Prototype #1	Prototype #2	Prototype #1	Prototype #2
R_1	1.915 mm	1.909 mm	1.917 mm	1.905 mm	1.912 mm
R_2	2.218 mm	2.225 mm	2.224 mm	2.180 mm	2.213 mm
R_3	2.296 mm	2.304 mm	2.311 mm	2.298 mm	2.301 mm
d_1	1.580 mm	1.587 mm	1.590 mm	1.582 mm	1.584 mm
d_2	1.123 mm	1.129 mm	1.130 mm	1.115 mm	1.119 mm
d_3	0.961 mm	0.965 mm	0.971 mm	0.952 mm	0.966 mm
t	550 μm	565 μm	620 μm	580 μm	635 μm

respectively. Therefore, the fabricated plastic devices with cavity size of about 2 mm should have shrunk about 13 μm at room temperature (hot embossing temperature at about 160 °C). On the other hand, the iris has thickness of only about 580 μm and should have shrunk for only 4 μm. The electroplating process will add another 8 μm on the surfaces. As a result, a net thickness increase of about 12 μm is expected. These anticipated variations are generally observed. Furthermore, it is noted that by using the same mold insert and same embossing process (temperature, pressure, etc.), the measured key dimensions of the plastic waveguide are within ±30 μm. Further improvements could be achieved by the following suggestions. First, thickness control of the electroplated gold could be achieved by optimizing electroplating conditions. Second, a better grinding/cleaning process should be introduced to reduce particle entrapment on the waveguide surfaces. Third, an integrated polymeric flange/waveguide manufacturing process could solve non-repeatability issues coming from gaps and tilt during the final press fitting assembly process.

The W-band scattering parameters $s11$ (return loss) and $s21$ (insertion loss) of the first prototype iris filters have been characterized (Agilent *PNA 5250* network analyzer). Fig. 5 shows the measured spectral responses from the first prototype with a passband between 93.7 GHz and 97.2 GHz. The simulation result is also shown for comparison by assuming perfect infinite conductivity for the electroplated gold surfaces. The measured results show a 3-dB bandwidth of 3.46 GHz (3.63%) centered at 95.4 GHz and a 20-dB bandwidth of 6.23 GHz (6.53%) and insertion loss at 96.13 GHz as −3.49 dB with the return loss as −15.86 dB. The measured rejection loss is better than 50 dB while simulated results show rejection more than 100 dB because the network analyzer has limited resolution in detecting low signal levels. The loaded quality factor for a single cavity resonator, Q_l, can be calculated as [16]:

$$Q_l = \frac{f_0}{\Delta f} \tag{1}$$

where f_0 is the center frequency and Δf is the 3-dB bandwidth. The loaded quality factor is calculated as 27.57. The unloaded quality

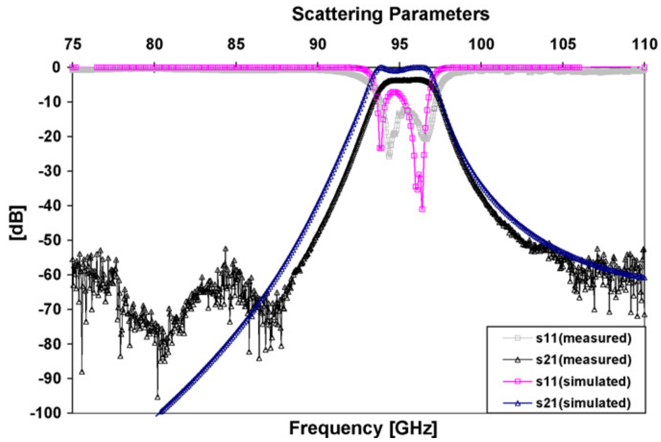

Fig. 5. Measured and simulated scattering parameters of the first prototype iris filter from 75 GHz to 110 GHz. At 96.13 GHz, the measured return loss parameter, $s11$, is -15.86 dB and the measured transmission loss parameter, $s21$, is -3.49 dB.

factor, Q_u, can be calculated from the relation between the insertion loss, IL, and the loaded quality factor [16]:

$$\left|\mathrm{IL}\right| = \frac{1}{1 - Q_l/Q_u} \tag{2}$$

Assuming five identical cavities, the unloaded quality factor for a single cavity resonator is calculated as 416.65.

Fig. 6(a) shows the measured and simulated responses of the second prototype filter and (b) is the close-up view on the passband between 90 GHz and 105 GHz. This filter shows a bandwidth of 3.05 GHz centered at 96.77 GHz while simulation predicts a bandwidth of 3.5 GHz centered at 96.63 GHz. This second prototype filter had a minimum insertion loss of -1.22 dB, a return loss better than 9.3 dB over the entire pass band, and a loaded quality factor 31.73, and an unloaded quality factor for a single cavity resonator is 1210.6. The shift in center frequency relative to the first prototype is due to the increase in iris thickness by 55 μm. Overall, the simulation and measurement results are in good agreement which indicates the effectiveness of design methodology and fabrication technique.

Many sources contribute to the differences between the simulation and experimental results such as misalignments between the prototype and the network analyzer, surface roughness of electroplated gold, the finite conductivity of gold (the measured dc conductivity using a 4-point probe is $1.5 \times 10^6\ \Omega\,\mathrm{m}^{-1}$), error in the iris dimensions, and the non-perfect round iris tips. We address some of the issues in this section. First, simulation results show slight downshift in center frequency due to the round tips as the average iris thickness becomes smaller. Second, rough surfaces result in less conductive sidewalls such that insertion loss increases as previously reported [17]. The effects of finite dc conductivity and gap between the filter and the network analyzer are simulated in

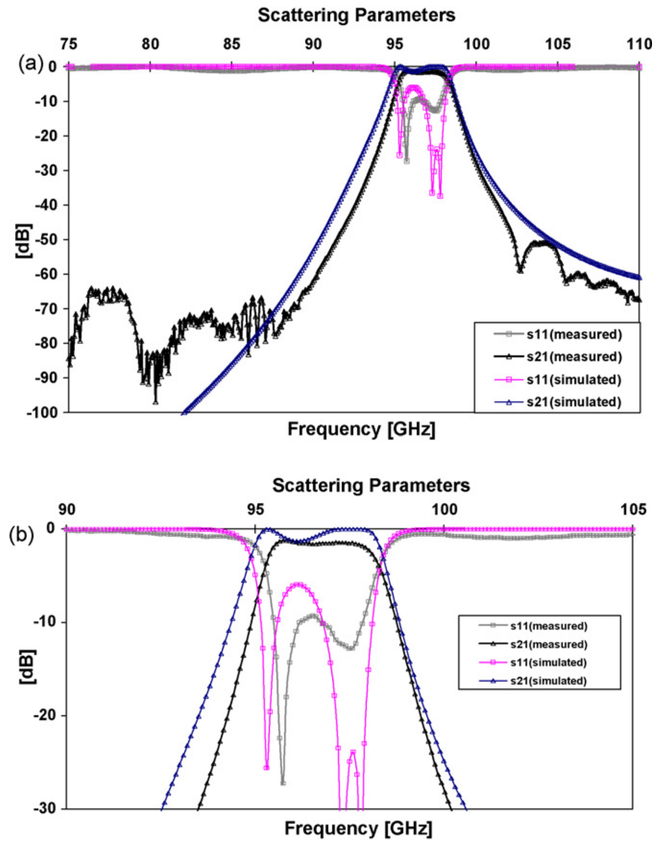

Fig. 6. Simulated and measured scattering parameters of the second prototype filter. (a) Filter measurement results over the entire W-band and (b) close-up view in the passband region.

Fig. 7. The ideal waveguide with infinite conductivity will have 0 dB in insertion loss and $-\infty$ dB in return loss (HFSS will show -80 dB). For finite sidewall conductivity at $1.5 \times 10^6\ \Omega\,\mathrm{m}^{-1}$, the non-zero insertion loss gradually reduces from 0.0212 dB/mm at 75 GHz to 0.0148 dB/mm at 110 GHz. On the other hand, the return loss shows better than 40 dB over almost the entire band (or less than 0.01% of the signal being reflected). Third, the possible gaps and tilt between the polymeric flange and waveguide devices [14] can be another source. Analysis is conducted by introducing a 50 μm-wide connecting gap between the filter and the network analyzer of a 1-in. long W-band waveguide. It is found that the 50 μm-wide gap will result in an additional transmission loss such that non-zero insertion loss of 0.0344 dB/mm at 75 GHz will gradually decreases to 0.0284 dB/mm at 110 GHz. The return loss, on the other hand, is mostly better than 30 dB (about 0.1% of the signal is reflected), which indicates the undesired 50 μm gap has a significant effect on increasing the return. The non-reproducibility and potential

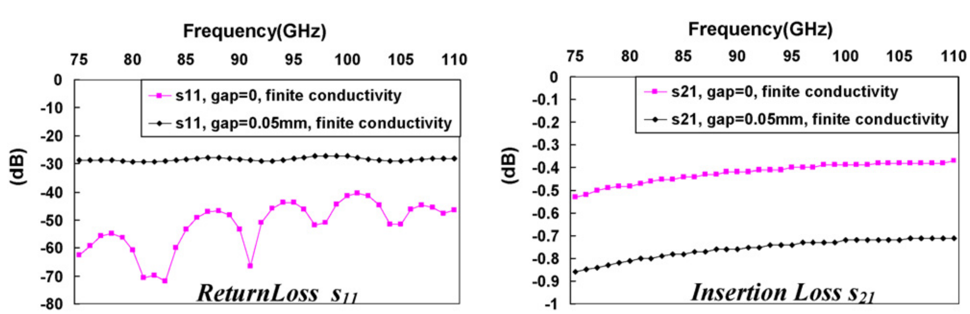

Fig. 7. Scattering parameters of a 1-in. long waveguide having sidewalls of $1.5 \times 10^6\ \Omega\,\mathrm{m}^{-1}$ conductivity and 50 μm-wide gap between the filter and the network analyzer.

measurement errors coming from gaps and tilt during press fitting process could be alleviated by implementing an integrated polymeric flange/waveguide manufacturing process. The relatively large insertion loss measured as −3.49 dB of first prototype filter may be attributed to the combined effects of both finite conductivity and gap between the filter and the network analyzer, while the second prototype filter has a better insertion loss measured as −1.22 dB at 95.83 GHz and agrees well with simulation value −1.01 dB, which attributes to the improvement of electroplating surface quality with more conductive sidewalls and decrease of insertion loss.

4. Conclusions

Plastic W-band iris filters have been demonstrated using the principle of Chebychev 5th-order polynomial design. HFSS simulations were conducted in order to study the effect of the iris thickness on the center frequency, bandwidth, and return loss of the filters. The rectangular waveguide iris filters have been fabricated using an inexpensive plastic hot embossing technique with a mold insert manufactured using electric discharge machining to achieve the required iris dimensions. A plastic flange was also integrated with the iris filter to help connecting the filter to the network analyzer. Two prototype filters were fabricated and measured using a PNA 5250 network analyzer from 75 GHz to 110 GHz. The lower and upper cutoff frequencies of the first iris filter were measured to be 93.7 GHz, and 97.2 GHz, respectively and the geometric mean center frequency was calculated as 95.4 GHz. At 96.13 GHz, the return and insertion losses were −15.86 dB and −3.49 dB, respectively. The out of band rejection was better than 50 dB and the bandwidth was 3.46 GHz (3.6% bandwidth), which corresponds to a loaded quality factor of 27.57 and an unloaded quality factor for a single cavity resonator of 416.65. The second filter had better performances with a bandwidth of 3.05 GHz (3.15% bandwidth) centered at 96.77 GHz, minimum insertion loss of −1.22 dB at 95.83 GHz, and a return loss of −18 dB. The out-of-band rejection was better than 60 dB, a loaded factor of 31.73 and an unloaded quality factor for a single cavity resonator of 1210.6. The shift in center frequency was attributed to the thicker irises in the second prototype.

Acknowledgements

This project is supported in part by a NSF grant DMI-0428884 and these devices were fabricated in the UC-Berkeley Microfabrication Laboratory and the Mechanical Engineering Machine Shop. The authors would like to thank Mr. Ron Wilson for taking the SEM pictures, Mr. John Morton from the Mechanical Engineering Department machine shop for fabricating the mold inserts, Professor J.C. Chiao of University at Texas, Arlington and Professors Jack Welch and Ali Niknejad at UC Berkeley for valuable discussions, and Mr. Bill Kwan from Agilent Technologies for his support on the experiments.

References

[1] Matthaei, Microwave filters, in: Impedence-matching Networks, and Coupling Structures, McGraw-Hill, 1964, pp. 421–519.
[2] J.R. Ried, E.D. March, R.T. Webster, Micromachined rectangular-coaxial transmission lines, IEEE Trans. Microwave Theor. Tech. 54 (2006) 3433–3442.
[3] R.T. Chen, E.R. Brown, C.A. Bang, "A compact low-loss Ka-band filter using 3-dimensional micromachined integrated coax," in: 17th IEEE International Conference on Micro Electro Mechanical Systems, pp. 801–804, Maastricht, The Netherlands, 2004.
[4] N. Asao, N. Yoneda, M. Mukuda, K. Yamasaki, O. Kamohara, Y. Yoshino, K. Henmi, Metal-plated plastic waveguide filter using injection molding process, in: 2003 IEEE MTT-S International Microwave Symposium Digest, vol. 2, 2003, pp. 941–944.
[5] C.Y. Chi, G. Rebeiz, A low-loss 20 GHz micromachined bandpass filter, in: IEEE MTT-S International Microwave Symposium Digest, vol. 3, New York, NY, 1995, pp. 1531–1534.
[6] S.V. Robertson, L.O.B. Katehi, G.M. Rebeiz, Micromachined self-packaged W-band bandpass filters, in: IEEE MTT-S International Microwave Symposium Digest, vol. 3, New York, NY, 1995, pp. 1543–1546.
[7] K. Jiang, M.J. Lancaster, I. Llamas-Garro, P. Jin, SU-8 Ka-band filter and its microfabrication, J. Micromech. Microeng. 15 (2005) 1522–1526.
[8] B.T. Lee, M.S. Kwon, J.B. Yoon, S.Y. Shin, Fabrication of polymeric large-core waveguides for optical interconnects using a rubber molding process, IEEE Photon. Technol. Lett. 12 (No. 1) (2000).
[9] L. Lin, Y.T. Cheng, C.-J. Chiu, Comparative study of hot embossed microstructures fabricated by laboratory and commercial environments, Microsyst. Technol. J. 4 (No. 3) (1998) 113–116.
[10] Liwei Lin, T.K. Shia, C.-J. Chiu, IC-processed plastic micropyramids for brightness enhancement, J. Micromech. Microeng. 10 (No. 3) (2000) 395–400.
[11] X.-J. Shen, Li-Wei Pan, Liwei Lin, Microplastic embossing process: experimental and theoretical characterizations, Sens. Actuators Phys. A 97–98 (2002) 428–433.
[12] Robert E. Collin, Foundations of Microwave Engineering, 2nd edition, McGraw Hill, 1992.
[13] F. Sammoura, Micromachined Plastic Millimeter-wave Radar Components, Ph.D. Dissertation, University of California at Berkeley, 2006.
[14] F. Sammoura, Y.C. Su, Y. Cai, C.-Y. Chi, B. Elamaran, L. Lin, J.-C. Chiao, Plastic 95-GHz rectangular waveguides by micro molding technologies, Sens. Actuators 127 (2006) 270–275.
[15] L.W. Pan, L. Lin, Batch transfer of LIGA microstructures by selective electroplating and bonding, IEEE/ASME J. Microelectromech. Syst. 10 (2001) 25–32.
[16] D.M. Pozar, Microwave Engineering, John Wiley & Sons, 1997.
[17] F.J. Tischer, Experimental attenuation of rectangular waveguides at millimeter wavelengths, IEEE Trans. Microwave Theor. Tech. MTT-27 (No. 1) (1979).

Biography

Firas Sammoura was born in Lebanon in 1980. He studied mechanical engineering at the American University of Beirut and earned his Bachelors of Engineering in 2001 with High Distinction. From 2001 until 2006, he was a student in the mechanical engineering department at the University of California at Berkeley. In May 2006, he received his PhD in the field of microelectromechanical systems. His dissertation was focused into building plastic millimeter-wave systems for Radar applications at 95 GHz. He was a student researcher with Hitachi Global Storage Technologies at the IBM Almaden Research Center where he did proprietary research in MEMS applications for the hard disk drive industry. From June till December 2006, he was a process development engineering staff at Cypress Semiconductors. In January 2007, he joined the Advanced Development Group in the Micromachined Product Division of Analog Devices in Cambridge, MA where he is currently a senior device characterization engineer for inertial MEMS products. Dr. Sammoura has two pending patent applications in the field of microwave engineering, one describing the design and fabrication of a 95 GHz phase shifter.